JOURNAL OF MATERIALS SCIENCE **35** (2000) 1009–1016

Rheology of injection-molded zirconia-wax mixtures

DEAN-MO LIU*‡
Materials Research Laboratories, Industrial Technology Research Institute, Chutung, Hsinchu, Taiwan 31015, ROC
E-mail: dean@ceramics.mmat.ubc.ca

WENJEA J. TSENG
Institute of Materials Science and Manufacturing, Chinese Culture University, Yan Ming Shan, Taipei, Taiwan 11114, ROC

Rheological behavior of highly-concentrated (with particle solids loading of 50–70 vol%) zirconia-wax mixtures was investigated. The particle surfaces were first modified by monolayer adsorption of stearic acid as a lubricant, followed by compounding with different fractions of low-molecular-weight wax. The mixtures roughly exhibit a pseudoplastic or Bingham behavior with a yield stress which increases exponentially with decreasing particle-particle separation. The maximum solid loading was determined experimentally to be 0.7, suggesting the particles arrange in an ordered dense packing configuration. Three models, namely, modified Elier's equation, Krieger-Dougherty equation, and Maron-Pierce equation were used to model the relative viscosity (η)-solid fraction (ϕ) relationship for the mixtures. The Krieger-Dougherty equation exhibits a good description on the mixture viscosity up to 65% solids concentration whilst the others are limited to 60% loading. Influence of temperature on mixture viscosity is critical particularly for higher solids concentration. For a 65% mixture, a pronounced particle-particle interaction dominates the mixture rheology at temperatures above approximately 75°C whilst below this temperature, the viscous flow of the organic vehicle turns to be important in dominating the mixture rheology. However, interparticle interaction becomes less significant when the solids concentration is below approximately 60%.

1. Introduction

Ceramic injection molding (CIM) has been known as an attractive forming technology permitting mass production of ceramic parts, associated with intricate geometry. Prior to molding, the ceramic particles of interest are blended homogeneously with organic binders of different characteristics, e.g., softening/melting points, in order of facilitate subsequent processing, e.g., debinding. The binders allow the solid particles to be freely moved under shear field of reasonable intensity during the transporting and molding processes.

In principle, a desired powder-polymer suspension for CIM requires relatively high solid concentration with suspension viscosity as low as possible at a given molding temperature. Both requirements ensure a high green-shape density with high degree of green microstructure homogeneity [1, 2] and of structural integrity [3]. Meanwhile, Suspensions with relatively high solids loading have a low content of binder, and this may facilitate its removal during debinding. To achieve the goal, numerous attempts have been reported to utilize a number of combinations of organic vehicles and particle characteristics, e.g., by adjusting particle size/size distribution or by particle surface modification via chem-/phys-adsorption, and some of them have indeed achieved satisfactory results [4, 5, 6].

The flow behavior of powder-polymer mixtures during molding can vary considerably due to wide variations in powder characteristics and organic vehicles employed. In view of the literature, alumina powders have been the most widely-used model material in demonstration of the CIM processes [2, 3, 5, 7, 8]. The powder loadings are typically in the range of 50–60 vol%. However, the moulding of fine zirconia powders, particularly when the solid loading is greater than 60 vol%, has not been extensively studies. The main purpose of this investigation is to characterize in detail the rheological behavior of the fine zirconia powder-wax mixture with relatively high solids fraction over a wide range of shear rates and working temperatures. A further characterization of injection molding parts will be conducted and discussed separately.

* Author to whom all correspondence should be addressed.

‡ *Present address:* Materials Science and Engineering Department, University of British Columbia, 309-6350 Stores Rd., Vancouver, BC V6T 1Z4, Canada.

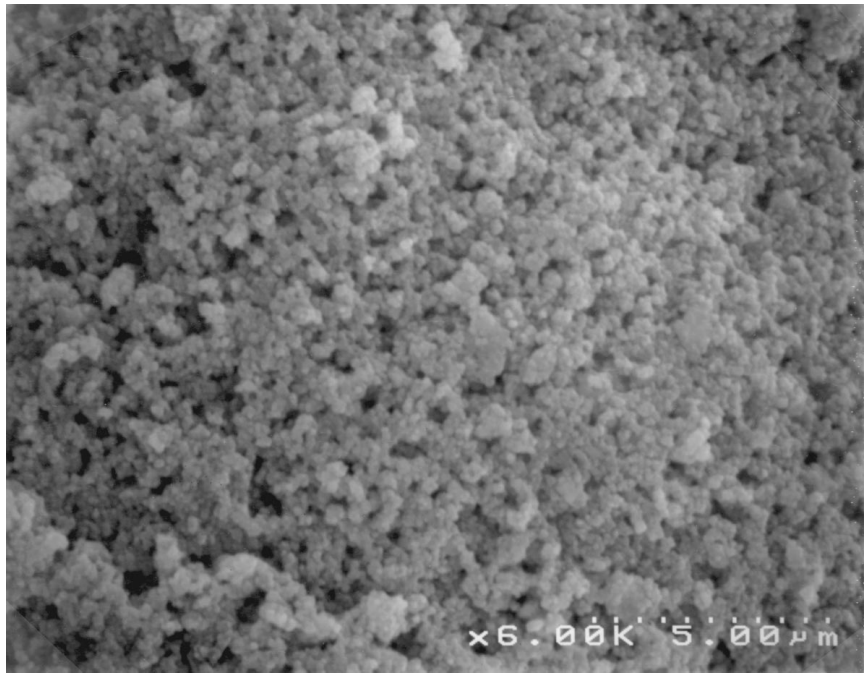

Figure 1 Morphology of the zirconia powder employed in this investigation.

2. Experimental procedure

Fine zirconia powder particles (0.24 μm in average particle size, Fig. 1) were first modified by adsorption of monolayer stearic acid as a stabilizing agent through an adsorption operation. The adsorption was performed by mixing varying amounts of the acid with the powder in toluene for 24 h. After separation of the adsorbed powder by filtration, the powder was washed with the solvent several times to ensure no residual acid, other than that adsorbed, being deposited onto the powder surface. Thermal gravimetric analyzer (Netszch, Model STA 903) was used to determine the adsorption isotherm of the acid on the solid surface. The minimum amount of the acid to reach saturation adsorption was then determined.

The coated powder was compounded with paraffin wax (a flowing point $\sim$55°C) in a high shear mixer for sufficient time period. The powder-wax mixtures containing particle solid loadings ranging from 50 to 70 vol% were prepared into a cylindrical geometry by compressing the granulated mixture at a suitable temperature for rheological measurement. The rheological behavior of the mixtures was first characterized at a fixed temperature of 58.5°C through a capillary rheometry (Shimadzu, CFT-500D). Further increase in the working temperature to 100°C was conducted in some selected mixtures. Two and in some case three runs were conducted for each powder-wax mixture to ensure the accuracy and reproducibility of the experiments.

3. Results and discussion

3.1. Adsorption behavior

Fig. 2 shows the adsorption isotherm of the organic acid onto the zirconia powder. The adsorption exhibits typically a Langmuir-type behavior with a saturation reached at a value of 1.495 mg/m^2, which is indicative of a complete monolayer surface coverage. Based on the adsorption isotherm, the effective surface area for a molecule of the stearic acid to be covered is calculated to be approximately 32 Å [2]. This molecular area is roughly of the same order of magnitude as the value of 44 Å [2] as if the acid molecule was oriented with both the carboxyl group and the double bond on the zirconia surface and with the hydrocarbon tail of the acid molecule extending into the solvent phase [9]. Strictly speaking, both the solvent power and particle surface characteristic dominates the resulting structure conformation of the adsorbed molecules. This may cause the adsorbed molecules to be oriented in a variety of ways with respect to the solid surface. However, available data on the system alike is rarely found. By analogy, Doroszkowski *et al.* [10] computed the molecular area of the minimum cross-section for an oleic acid and obtained a value of 29 Å [2]. This area is in good

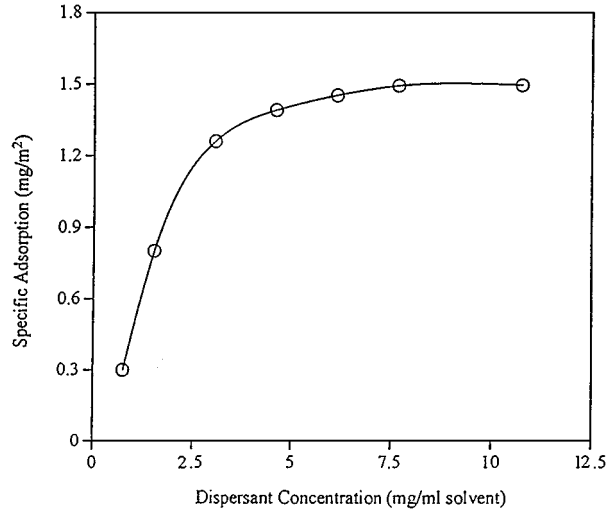

Figure 2 Adsorption isotherm of the stearic acid onto zirconia particle.

agreement with the molecular area determined experimentally for the stearic acid and this suggests the acid molecules were adsorbed in a normal orientation onto the particle surface via the carboxyl group.

The thickness of the adsorbed layer has its fundamental importance in characterizing the adsorption behavior and subsequent efficacy on effective solid fraction, although the adsorbed layer thickness is not a primary concern in this investigation. In brief, the thickness of the adsorbed layer is determined via a conventional viscometric technique through the use of dilute suspensions (solids loading of 0.85–2.5 vol%). The effective solid fraction is accordingly increased due to the adsorption. In this case, an incremental solids fraction by approximately 7.6% is determined, which follows the calibration from Einstein's equation, i.e., $\eta = 1 + 2.5\ \phi$ where η is the relative viscosity and ϕ is the solid fraction, as had been done by Rowland *et al.* [11]. This corresponds to a calculated thickness of the adsorbed stearic acid layer on the zirconia particles to be about 30 Å. This thickness is nearly identical to the chain end-to-end length of the stearic acid molecule, 24 Å, calculated by Doroszkowski *et al.* [10]. This finding provides additional support for previous discussion on the structural conformation of the acid molecule once adsorbed onto the zirconia surface. This adsorption increases the effective solids loading over the studied range from 53.8 (corresponding to a starting loading 50%) to 75.3 vol% (70%). However, in the forthcoming discussion on mixture rheology, the original particle solid fraction is employed as the primary parameter for analysis.

3.2. Effect of solid loading

On determining the rheological behavior of the mixtures, one of the relatively important parameters is the determination of maximum solid loading (ϕ_m) that can be achieved at a given powder-polymer system. In general, a broader size distribution for spherical particles enables the achievement of high ϕ_m [12, 13]. In this study, the particles employed are roughly spherical in shape and are likely to be uniformly distributed in size as visually observed in Fig. 1. However, the particle size determined from the analyzer (Fig. 3) indicates a wider distribution over the range of 0.1–1 μm than visually observed. The larger particles detected by the analyzer suggests the presence of some particle agglomerates, which would be detrimental to particle dispersion and reduce the maximum attainable value of ϕ_m. However, from a qualitative observation on the viscosity measurement, the mixture with solids loading only greater than 65 vol%, e.g., 68%, shows an increasingly difficult in flow behavior and no flow occurs at 70% loading even under the maximum shear stress, ~50 MPa, available to the capillary rheometer. The maximum solids loading is therefore determined to be ~70% in this case. This value suggests that an ordered dense packing of the particles may be achieved in current powder-wax system. For a reliable analysis, a subsequent discussion on the effect of solid loading will be focused over the range of 50–65%.

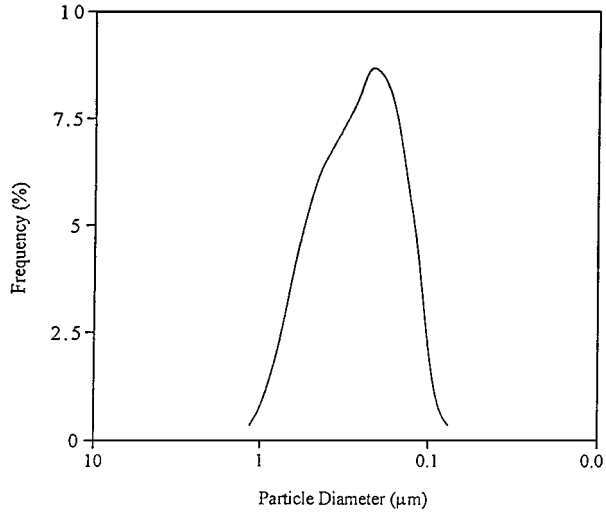

Figure 3 Particle size distribution of the zirconia powder employed in this investigation.

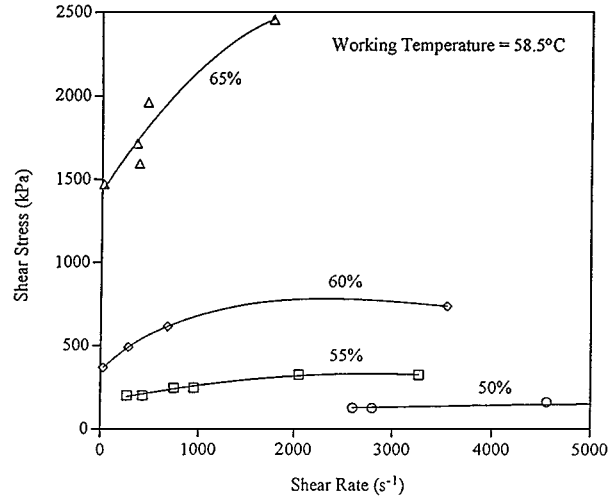

Figure 4 Shear stress-shear rate curves for the mixtures of different solids loading at 58.5°C.

3.2.1. Yield stress

Fig. 4 shows the non-linear shear rate-shear stress curves of the powder-wax mixtures for differing solid fractions (ϕ) at a working temperature of 58.5°C. Strictly speaking, the mixtures do not show Bingham-like behavior, particularly when $\phi \geq 55\%$. However, an alternative expression using the (shear stress, $\tau)^{1/2}$ versus (shear rate, $\gamma)^{1/2}$ plot shows a linear relationship with correlation coefficients greater than 0.94 for all the mixtures. According to the equation derived by Casson [14],

$$\tau^{1/2} = \tau_y^{1/2} + (\eta \cdot \gamma)^{1/2} \quad (1)$$

the yield stress (τ_y) can be evaluated from the intercept value of the $\tau^{1/2} - \gamma^{1/2}$ line for each mixture. The obtained yield stress has a value of 0.08 MPa for 50% mixture and increases by 4.6 times with increasing solids loading to 60% and becomes sharply increased by about 16 times when ϕ is reached at 65%. Although, from a debinding viewpoint, a higher yield stress may ensure a shape retention during thermal debinding of injection-molded parts, it may not be favorable for a

desirable rheology in injection molding operations [15]. Therefore, we believe that the rheological behavior for solids loading below approximately 60% may be an acceptable level for CIM when the working temperature is at 58.5°C. In fact, an increase in working temperature should be useful in facilitating the injection operation for mixtures with a higher solid loading by reducing viscosity of the mixture and will be discussed later.

Since the yield stress can be considered as the minimum force required to make a relative movement between particle assemblies, the greater value of the yield stress due to higher solids concentrations suggests a greater stress imposed by the solid phase upon the mixture. Factors such as geometrical interlocking and particle-to-particle attraction may become increasingly important when solid concentration is increased. Both factors imply the importance of particle-particle separation which is indeed a reflection of a measure of interparticle potential. If this argument is true, then, the minimum stress to initiate particle movement can be related in a physically meaningful way to the interparticle spacing, although it frequently correlates with solid fraction in the literature [16]. The average interparticle spacing (λ) can be related to the solids fraction (ϕ) by [17],

$$\lambda = \frac{4}{3} r \frac{1-\phi}{\phi} \tag{2}$$

where r is the average particle radius, i.e., 0.12 μm in this case. A plot of the yield stress versus interparticle spacing (including the previously-mentioned adsorption effect) through least-squares fitting yields a better correlation coefficient (0.985) in terms of an exponential function (Fig. 5) than versus solids fraction (0.969). This comparison seems to support the presumed argument and further suggests the importance of particle-particle interaction either due to mechanical interlocking or due to attractive force on the resulting yield stress.

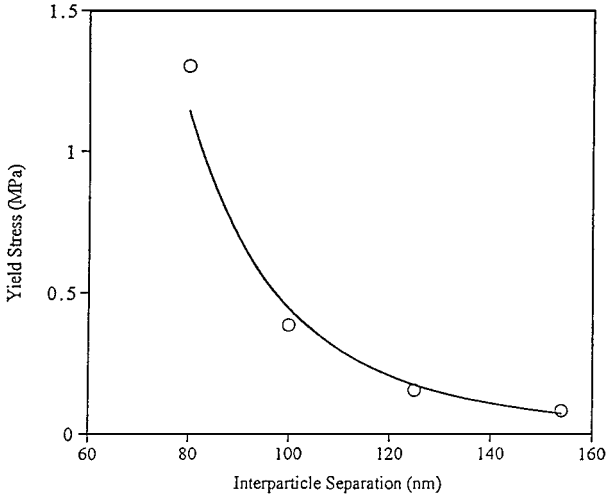

Figure 5 Yield stress of the mixture as an exponential function of interparticle separation.

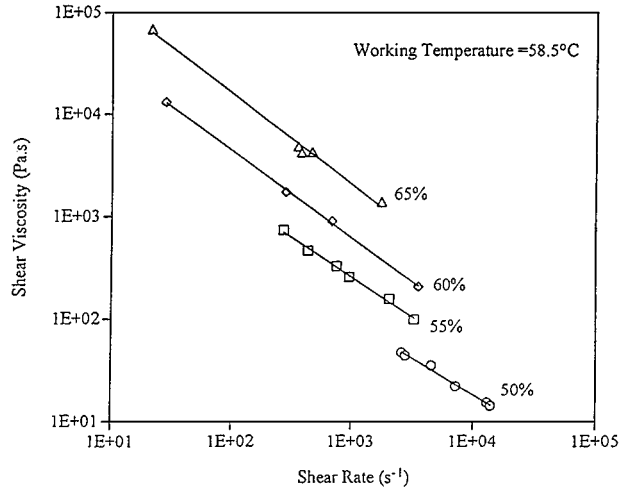

Figure 6 Shear viscosity of the mixture decreases linearly with increasing shear rate on a log-log plot, indicating a pseudoplastic flow behavior.

3.2.2. Shear viscosity

Fig. 6 shows the shear viscosity (η_s) of the mixtures at a working temperature of 58.5°C as a linear function of shear rate ($\dot{\gamma}$) over the range of approximately 20–15,000 s^{-1} on a log-log plot. Such linearity approximates a pseudoplastic character of the mixtures and accordingly can be expressed by

$$\eta_s = K\dot{\gamma}^{n-1} \tag{3}$$

where K represents the fluid consistency index and n is the power-law flow index. For a Newtonian fluid, $n = 1$, the shear viscosity is independent of shear rate. In present cases, the index n decreases with increasing solids loading and fall between 0.1–0.28 at 58.5°C. The decrease in the flow index n with increasing solids loading indicates an increasing non-linearity in flow behavior. This increase in non-linear flow behavior with increasing solids fraction may be originated from alignment of particle clusters or particle layers when a considerable volume fraction of the system is occupied by rigid solid phase. As revealed in Equation 3, at higher solid concentrations, the shear viscosity of the mixture exhibits a greater shear-rate dependence (lower $n-1$ value) than that at lower solids concentration over the shear rate range of study. This greater shear-rate dependence may be considered as a result of a greater dependence of energy dissipation upon increasing solids concentration. If the above arguments are correct, it may suggest that the solids concentration may be correlated with the power-law index n (or in a form of $(n-1)$ in Equation 3), and surprisingly, a well-fitted straight line (with correlation coefficient = 0.989) is obtained as depicted in Fig. 7. On this basis, it may be reasonable to hypothesize that the non-linearity of the flow behavior of the mixture due to the presence of solid phase is linearly dependent upon the concentration of the solid phase. (In fact, such non-linearity in flow behavior of the mixture becomes less pronounced when the working temperature is increased to a certain critical level as will be discussed later.)

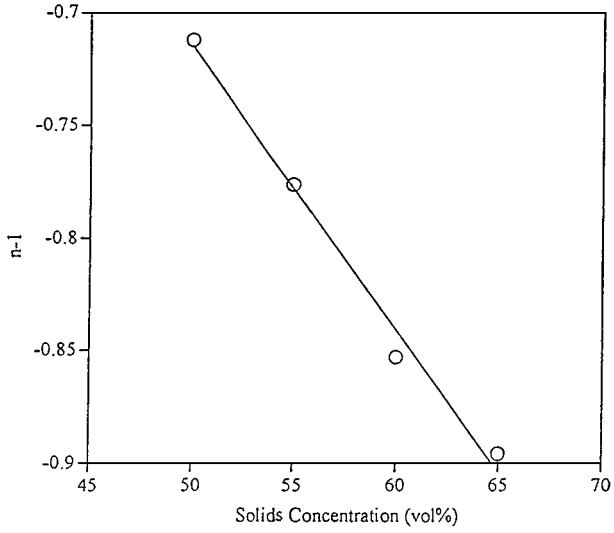

Figure 7 The power-law flow index of the mixture as a linear function of the solid concentration.

3.2.3. Model fitting

The influence of solids concentration on dispersion rheology has long been an interesting and important subject for many researchers. A number of theoretical as well as empirical equations have been developed to predict the rheological behavior of concentrated suspensions [18, 19]. Each equation has achieved some agreement between prediction and measurement, but with limits to factors such as solids concentration and powder characteristics, in a variety of suspension systems. For the highly concentrated powder-wax systems employed presently, three models were utilized in order to compare in more detail of the mixture rheology. The first model is written as,

$$\eta = \left[1 + \frac{[\eta]\phi\phi_{\mathrm{m}}}{m(\phi_{\mathrm{m}} - \phi)}\right]m \tag{4}$$

which is a modified Eiler's derivation [20]. The value $m = 2$ at high shear rate and will be used for data fitting in this case because the shear rate for CIM is frequently high.

The second is the well known Krieger-Dougherty equation [21] which is generally suitable for concentrated suspensions,

$$\eta = \left[1 - \left(\frac{\phi}{\phi_{\mathrm{m}}}\right)\right]^{-[\eta]\phi_{\mathrm{m}}} \tag{5}$$

The third one is probably the best empirical expression, as claimed by a number of researchers, with a very simple form [22]

$$\eta = \left[1 - \left(\frac{\phi}{\phi_{\mathrm{m}}}\right)\right]^{-2} \tag{6}$$

All the parameters used in these equations have the same physical meaning; η is the relative viscosity (defined as the mixture viscosity divided by the viscosity of the carrier fluid, i.e., wax), $[\eta]$ is the intrinsic viscosity, ϕ is the particle solids loading, and ϕ_{m} is the maximum solid loading and is experimentally determined to be 0.7.

Among these equations, except that of Equation 6, only one unknown parameter, i.e., intrinsic viscosity $[\eta]$, has to be determined in order to obtain a numerical form capable of describing the rheological behavior of the powder-wax mixture. These equations were first expressed in a linearized form and then Equation 4 becomes,

$$\eta^{1/2} = 1 + \frac{[\eta]\phi\phi_{\mathrm{m}}}{2(\phi_{\mathrm{m}} - \phi)} \tag{7}$$

and Equation 5 becomes,

$$\ln\eta = -[\eta]\phi_{\mathrm{m}} \ln\left(1 - \frac{\phi}{\phi_{\mathrm{m}}}\right) \tag{8}$$

From the linearized form of Equation 7, the intrinsic viscosity can be determined using a $\eta^{1/2}$ versus $\phi/(\phi_{\mathrm{m}} - \phi)$ plot with a slope equal to 0.35 $[\eta]$ and an intercept value of unity. The relative viscosity used to characterize Equation 7 was obtained by extrapolating the shear rate ($\dot{\gamma}$) to infinity at which the value $\dot{\gamma}^{1/2} = 0$ in a $\ln\eta - \dot{\gamma}^{1/2}$ plot as similarly done by Doroszkowski *et al.* [9]. Fig. 8 shows the linear relation of Equation 7. The intrinsic viscosity has a value of 2.946. Apparently, large deviations appear as the solids loading becomes greater than 60 vol% and this would limit the predictive capability of Equation 4 to a mixture with a limiting loading of 60%. Similarly, a $\ln\eta$ versus $\ln(1 - \phi/\phi_{\mathrm{m}})$ plot from Equation 8 yields a line of slope equal to $-[\eta]\ \phi_{\mathrm{m}}$ with the intercept through the origin, as illustrated in Fig. 9. The intrinsic viscosity obtained from Fig. 9 is 3.044 which is close to the value computed from Fig. 8. Furthermore, the straight line shown in Fig. 9 reveals that the use of Equation 5 enables prediction of mixture rheology over the entire solid concentration range of study, 50–65 vol%.

Plugging the available parameters into Equations 4 and 5 a comparison can be made between the calculated (from these equations) and measured relative

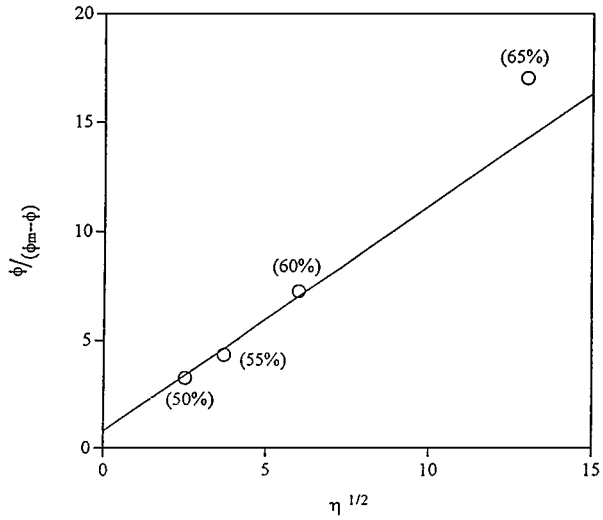

Figure 8 A $\eta^{1/2}$ versus $\phi/(\phi_{\mathrm{m}} - \phi)$ plot according to the linearized form of Equation 7.

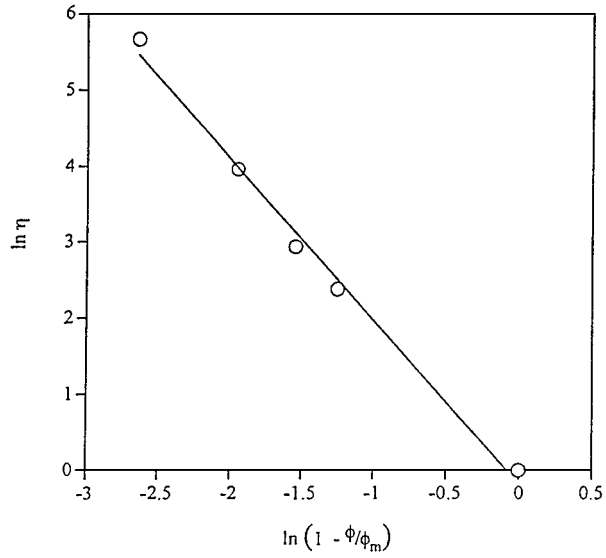

Figure 9 A $\ln(1-\phi/\phi_m)$ versus $\ln\eta$ plot according to the linearized form of Equation 8.

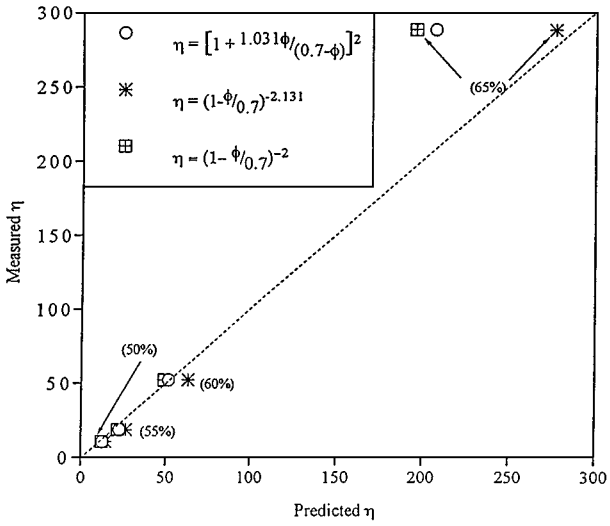

Figure 10 A comparison between the calculated and the experimentally-measured relative viscosity of the mixtures.

viscosities. Fig. 10 shows the resulting comparison, together with the data calculated directly from Equation 7. As expected, the experimentally-determined Krieger-Dougherty equation provides good data fitting for the powder-wax mixtures over the solid loading range of 50–65%, whereas the other two equations describe the mixture rheology well only at solids loading below approximately 60%. The discrepancy in rheological prediction among these equations at 65% loading may probably arise from the predictive nature and sensitivity to, for instance, the wax distribution, of the equation itself. The reason for the authors to take the wax distribution effect into account is due to the fact that at some high level of solids concentration, e.g., 65 vol%, the wax may distribute as a layer of coating, having an average thickness of 80 nm according to Equation 2, on the particles and some pore-like pockets may appear among the coated particles [7]. Under such conditions, the uniformity of wax distribution may be easily altered widely in scale as compared to those mixtures having a higher wax content. These factors may

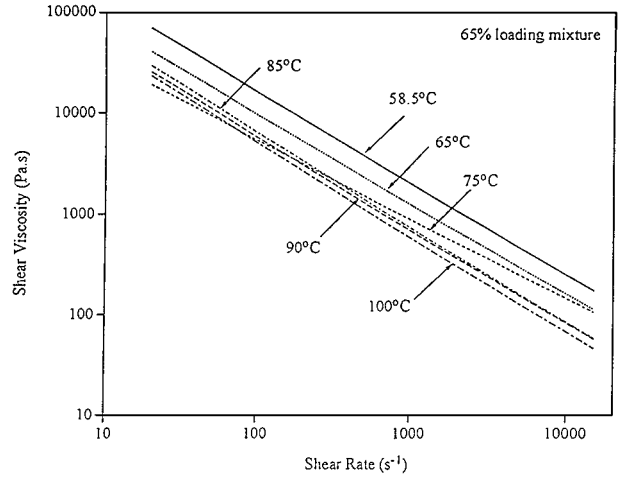

Figure 11 Shear viscosity versus shear rate plot for 65% mixture over temperature ranges of 58.5°C–100°C.

be responsible for the observed discrepancy. In other words, it may be assumed from current understanding that the numerical form of Krieger-Dougherty equation shows little affect on wax distribution (or other possible factors), whilst the others are likely to be more sensitive.

3.3. Effect of working temperature

Fig. 11 shows the shear rate ($\dot{\gamma}$)-shear viscosity (η_s) lines on a log-log plot for 65% mixture at temperature range of 58.5°C–100°C. The shear viscosity of the mixture (η_s) decreases with increasing working temperatures and particularly pronounced at shear rate greater than about 800 s^{-1}. This decrease in mixture viscosity with increasing temperature is due to the variation of wax viscosity (η_0) with temperature which is generally given by;

$$\eta_0 = A \exp\left(\frac{-E_v}{RT}\right) \tag{9}$$

where A is constant, R is the gas constant, and E the activation energy for viscous flow.

It is interesting to note that the $\dot{\gamma} - \eta_s$ lines in Fig. 11 exhibit different values of slope, or more specifically, different degrees of shear-rate dependence by having different values of power-law flow index. This also indicates that the mixture becomes more non-Newtonian, i.e., an increasing n or a decreasing $(n-1)$ value, as the temperature is increased. Figs 12a and b illustrate the mixture viscosity against temperature for 60% and 65% mixtures at different shear rates. The shear viscosity is in general decreased with both increasing temperature and shear rate, with the exception that an anomalous increase in viscosity for 65% mixture at shear rates below 1000 s^{-1} is observed when the temperature is greater than 75°C. However, this is not that obvious for 60% mixture. Since the flow behavior of the mixture under shear is dependent upon the hydrodynamic interaction between the particles and the molten wax, and the particle mobility in the molten wax is also affected by the viscosity of the molten wax, a decrease in wax viscosity

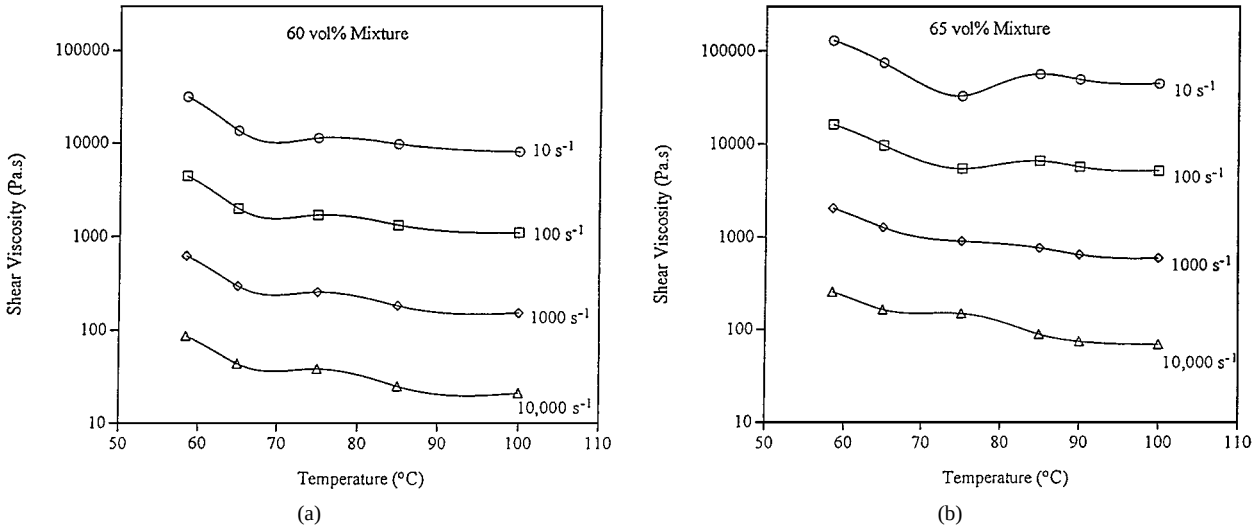

Figure 12 Shear viscosity as a function of working temperature for (a) 60% and (b) 65% mixtures at shear rates of 10 s^{-1}, 100 s^{-1}, 1000 s^{-1}, and 10,000 s^{-1}.

due to temperature rise may induce an increment of interparticle interaction. This anomalous increase in shear viscosity at higher temperature is therefore believed to originate from an increasingly pronounced interparticle interaction, particularly when the solids concentration is high. The viscous force (or hydrodynamic interaction) is comparatively lower than the interparticle interaction when the wax becomes less viscous at some critical temperature. Under such condition, a weakly-bonded particle network may be developed and cause an increase in mixture viscosity. This formation of a particle network suggests some degree of instability of the mixture and this appears to be consistent with an earlier observation by Johnson *et al.* [23], who suggested that the adsorption of stearic acid does not produce a stable suspension since the molecules are not long enough for an effective steric stabilization.

When the shear is high enough, the particle network collapses rapidly and the mixture rheology follows the viscous flow behavior of the wax (Fig. 12). In contrast, a higher wax viscosity at lower temperatures would reduce the particle-particle interaction appreciably and the mixture rheology is typically a result of the viscous flow behavior of the wax. Therefore, we believe that such an effect of insufficient steric stabilization, if it does exist in the present system, can surely be minimized by further adsorption of the wax molecules [24] during mixture preparation or by adjusting processing parameters, e.g., solid concentration, temperature, and shear field. Accordingly, the activation energy (E_v) for the viscous flow can be estimated through Equation 9 as shown in an alternative way in Fig. 13, a plot of log viscosity versus the temperature at a constant shear rate of 100 s^{-1}. The similarity in slopes for the mixtures containing 55, 60, and 65% solids, corresponding to an activation energy E_v of approximately 15.2 Kcal/mole over temperature range of 58.5–75°C, indicates the activation energy for the viscous flow is similar.

Since the power-law flow index n in Equation 3 defines the rheological nature of a given suspension system, it may be of considerable interest if the index n can be expressed as a function of temperature

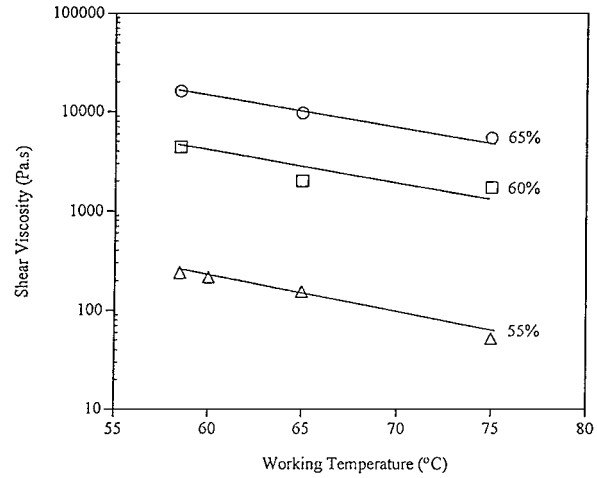

Figure 13 Effect of temperature over the range of 58.5°C–75°C on shear viscosity at a constant shear rate of 100 s^{-1} for 55%, 60%, and 65% loading mixtures.

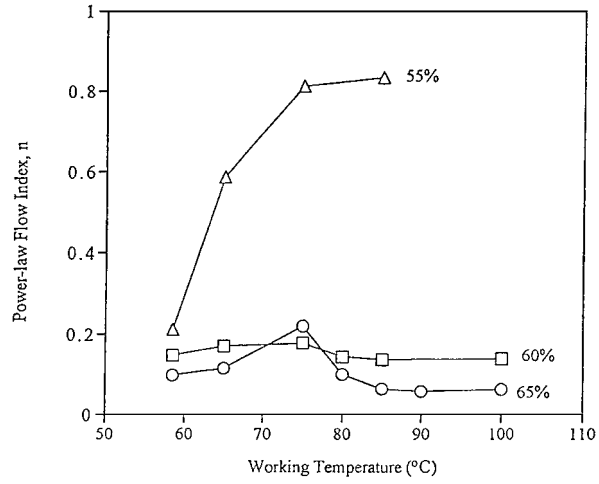

Figure 14 Effect of temperature on the power-law flow index n for the 55%, 60%, and 65% loading mixtures.

and Fig. 14 shows the resulting curves for 55%, 60% and 65% mixtures. At temperatures below about 75°C, the index n increases with increasing temperature, followed by a sharp decrease to a nearly constant value

when the temperature is greater than about 85°C for the both 60% and 65% mixtures. However, for a 55% mixture the index n rapidly increases up to 75°C, followed by a slow increase to 85°C. The increase in index n qualitatively indicates the tendency towards Newtonian ($n = 1$) flow behavior, particularly for the 55% mixture which exhibits an almost Newtonian flow character. However, for 60% and 65% mixtures, the sharp decrease in the index n suggests the mixture becomes more non-Newtonian with an increased shear viscosity as revealed in Fig. 12a resulting from intensive interparticle interaction may provide a reasonable explanation. For practical considerations, mixtures with solids concentrations greater than 60% are undesirable for injection molding at temperatures higher than about 75°C primarily because of a greater tendency for particle network formation, would probably occur, which tends to destabilize mixture structure and increase inhomogeneity in wax distribution during the operation.

It should be noticed from the above discussion that a critical interparticle spacing, corresponding to a balance between the hydrodynamic and the interparticle interactions, is likely to exist. Any particle-particle separation greater than the critical value may ensure a viscous flow rheology as can be seen for 55% mixture and the effect of particle-particle interaction should be minimized or neglected. However, before a theoretical derivation can be carried out (which is beyond the scope of present study), the critical spacing is approximately on the order of 100 nm (for 60% solids concentration including the adsorbed layer) according to the present experimental observations. This separation however may not be a universal value and is believed to be dependent upon a variety of chemical and physical aspects of the solid-liquid systems employed.

4. Conclusion and implication

The rheological behavior of zirconia-wax injection-molded mixtures has been investigated in terms of solids concentration (50–70 vol%) and working temperatures (58.5–100°C), over a wide range of shear rates from 20 s^{-1} to 15,000 s^{-1}. Experimental results show that the yield stress of the mixture increased exponentially with interparticle spacing at a given temperature. A high value of yield stress may ensure shape retention of the molded parts during subsequent thermal processing. The relative viscosity of the mixtures is an exponential function of solids loading and can be well-described by the Krieger-Dougherty equation up to solids concentrations as high as 65%. The influence of temperature on mixture viscosity is critically important in determining the possible rheology-dominating mechanism. In this case, the mixture rheology shows a viscous flow behavior with the wax viscosity decreasing exponentially with temperatures over the temperature range of 58.5–75°C. However, above 75°C, an increasing interparticle interaction (for 65% mixture) appears to dominate the mixture rheology and a similar (more non-linear) flow behavior is likely to occur at 85–100°C.

Based on the current observations, it implies that the control of mixture rheology, e.g., by temperature, is essentially critical for successful injection molding operation particularly when the solids loading are relatively high (e.g., >60 vol%) and the powder particles used are relatively small (e.g., 0.24 μm or smaller). An optimal temperature control appears to play a crucial role in dominating the flow behavior for highly concentrated mixtures. A temperature should not be too low for a reduction in transporting and molding capability due to high mixture viscosity or too high for an increasing interparticle interaction (this can be particularly pronounced when the particle size and interparticle spacing are small), resulting in a more non-Newtonian flow behavior, and in this case, a temperature below approximately 75°C may be suitable for the CIM operation.

Acknowledgement

The authors are gratefully indebted to the Minister of Economic Affairs, Taiwan (ROC) for supporting this research work under contract no. 873KG2220.

References

1. D. M. LIU and W. J. TSENG, *J. Mater. Sci.* **32** (1997) 6475–6481.
2. R. RUMAN, W. SLIKE and R. M. GERMAN, *Adv. Powder Metall. Part. Mater.* **5** (1993) 1–16.
3. M. J. EDIRSINGHE and J. R. G. EVANS, *J. Mater. Sci.* **22** (1987) 2267–2273.
4. T. KRAMER and F. F. LANGE, *J. Amer. Ceram. Soc.* **77**(4) (1994) 922–928.
5. S. NOVAK, K. VIDIRIC, M. SAJKO and T. KOSMAC, *J. Europ. Ceram. Soc.* **17** (1997) 217–223.
6. S. M. WOLFRAM and J. J. PONJEE, *J. Mater. Sci. Lett.* **8** (1987) 607.
7. M. TAKAHASKI, S. SUZUKI, H. NITANADA and E. ARAI, *J. Amer. Ceram. Soc.* **71**(12) (1988) 1093–1099.
8. B. C. MUSTSUDDY, *Proc. Br. Ceram. Soc.* **33** (1983) 117–137.
9. A. DOROSZKOWSKI and R. LAMBOURNE, *J. Colloid Interface Sci.* **26** (1968) 214–221.
10. *Idem., J. Polym. Sci. Polymer Symposia* **34** (1971) 252–263.
11. F. ROWLAND, R. BULAS, E. ROTHSTEIN and F. R. EIRISH, *Ind. Eng. Chem.* **57**(9) (1965) 46–52.
12. T. DABAK and O. YUCEL, *Rheol. Acta.* **25** (1986) 527–533.
13. J. A. MANGELS and R. M. WILLIAMS, *Amer. Ceram. Soc. Bulletin* **62**(5) (1983) 601–606.
14. N. CASSON, in "Rheology of Disperse Systems," edited by C. C. Mill (Pergaman Press, London, 1959) pp. 84–104.
15. M. J. EDIRISINGHE, H. M. SHAW and K. L. TOMKINS, *Ceram. International* **18** (1992) 193–200.
16. T. KATAOKA, T. KITANO, M. SASAHARA and K. NISHIJMA, *Rheol. Acta.* **17** (1978) 149–155.
17. M. K. AGARWALA, B. R. PATTERSON and P. E. CLARK, *J. Rheol.* **36**(2) (1992) 329–334.
18. R. N. WELTMANN and H. GREEN, *J. Appl. Phy.* **14** (1943) 569–576.
19. J. W. GOODWIN, *J. Colloid Sci.* **7** (1975) 246–293.
20. H. EILER, *Kolloid-Z* **97** (1941) 313–321.
21. P. C. HIEMENZ and R. RAJAGOPALAN, "Principles of Colloid and Surface Science," 3rd ed. (Mercel Dekker Inc., 1997) p. 169.
22. T. KITANO, T. KATAOKO and T. SHIROTA, *Rheol. Acta.* **20** (1981) 207–209.
23. R. E. JR. JOHNSON and W. H. MOSSISON, *Adv. Ceram.* **21** (1987) 323–348.
24. D. M. LIU, unpublished work.

Received 16 March 1998
and accepted 9 April 1999